









Cite this: *RSC Adv.*, 2017, 7, 32786

# Synthesis and characterization of innovative poly(lactide-co-glycolide)-(poly-L-ornithine/fucoidan) core-shell nanocarriers by layer-by-layer self-assembly

Jingqian Fan, <sup>a</sup> Yuangang Liu, <sup>\*abc</sup> Shibin Wang, <sup>abc</sup> Yulu Liu, <sup>a</sup> Siming Li, <sup>a</sup> Ruimin Long, <sup>a</sup> Ran Zhang <sup>a</sup> and Ranjith Kumar Kankala <sup>abc</sup>

Layer-by-Layer (LbL) self-assembly of nanocarriers has garnered the interest of researchers for a wide variety of biomedical applications. In this study, we demonstrated the preparation of poly(lactide-co-glycolide) (PLGA)-(poly-L-ornithine (PLO)/fucoidan)<sub>4</sub> core-shell nanoparticles (LbL NPs) by a LbL-based self-assembly process, which possessed a mean size of 170 nm. In LbL NPs, a drug carrying PLGA nano-core is coated with alternating PLO and sulfated polysaccharide fucoidan composite films as a shell on the surface. The anti-tumor drug doxorubicin (DOX) loaded into the PLGA core, resulted in better encapsulation efficiency and its *in vitro* release from LbL NPs demonstrates that this core-shell strategy takes an advantage of its ability to hold the drug cargo and exhibit controlled release. Further, *in vitro* cell uptake studies by confocal laser scanning microscopy (CLSM) examination in breast tumor cells (MCF-7 cell line) have confirmed that the nanocarriers are successfully internalized and outlined their presence in the cytoplasm after 4 h of incubation. These intracellularly delivered DOX-loaded LbL NPs exhibited significant anti-tumor activity against breast tumor cells. This innovative chemotherapeutic design taking above advantages of successful internalization along with controlled release property signifies as a promising interventional therapeutic delivery system.

Received 2nd May 2017  
Accepted 23rd June 2017

DOI: 10.1039/c7ra04908k

rsc.li/rsc-advances

## 1. Introduction

Layer-by-layer (LbL) self-assembly is one of the deposition techniques uses the basement to alternately adsorb two or more polyvalent materials in the polymer solution through electrostatic interactions.<sup>1</sup> Kotov *et al.* had made a significant contribution towards this process, by demonstrating a versatile method of LbL self-assembly of polycations and semiconductor nanoparticles (NPs) into stable ultrathin films.<sup>2</sup> Decher also made an important breakthrough in this technology using ionized polyelectrolytes *i.e.*, poly(styrene sulfonate) and poly(allylamine hydrochloride) deposited as multi-layers through electrostatic attraction on the solid base.<sup>3</sup> The preparation method is so simple as it depends on precise stoichiometry to prepare multi-layer coatings by a complex chemical reaction, and convenient, because it does not require any sophisticated equipment. Functional thin films could be generated by the LbL self-assembly method after adsorption on solid surfaces. Meanwhile, assembling an LbL system may exploit hydrophobic interaction,

hydrogen binding and van der Waals forces, which influence the stability, morphology and thickness of the films.<sup>4</sup> These films have been approved for various applications including the biological sensing, drug and gene delivery, regenerative medicine, tissue engineering and bionic medicine. Because of the mild reaction conditions and high drug-loading capability, LbL drug carriers have been applied as a new drug delivery system in nanomedicine research.<sup>5–7</sup>

This self-assembly technology combines different polyelectrolyte materials to construct an ultrathin carrier with multi-layer membrane structure. According to the source of the materials, the polyelectrolyte materials are classified into different categories, including synthetic and natural type polyelectrolytes.<sup>8</sup> Herewith, we designed the shell LbL assembly using two functional polymers *i.e.*, poly-L-ornithine (PLO) and fucoidan. PLO (Fig. 1a) is a biocompatible and low immunogenic polyelectrolyte,<sup>9</sup> within a primary amine side chain and charged when exposed to physiological environment, similar to poly-L-arginine, poly-L-lysine.<sup>10</sup> PLO possesses a wide variety of biological activities, such as enhancing the proliferation, migration and neuronal differentiation/regeneration responses of neural stem/progenitor cells, and also enhances the nasal absorption of hydrophilic macromolecular drugs.<sup>11–14</sup> PLO also holds good mechanical properties and enhances drug

<sup>a</sup>College of Chemical Engineering, Huaqiao University, Xiamen, 361021, China. E-mail: ygliu@hqu.edu.cn

<sup>b</sup>Institute of Pharmaceutical Engineering, Huaqiao University, Xiamen, 361021, China

<sup>c</sup>Fujian Provincial Key Laboratory of Biochemical Technology, Xiamen, 361021, China



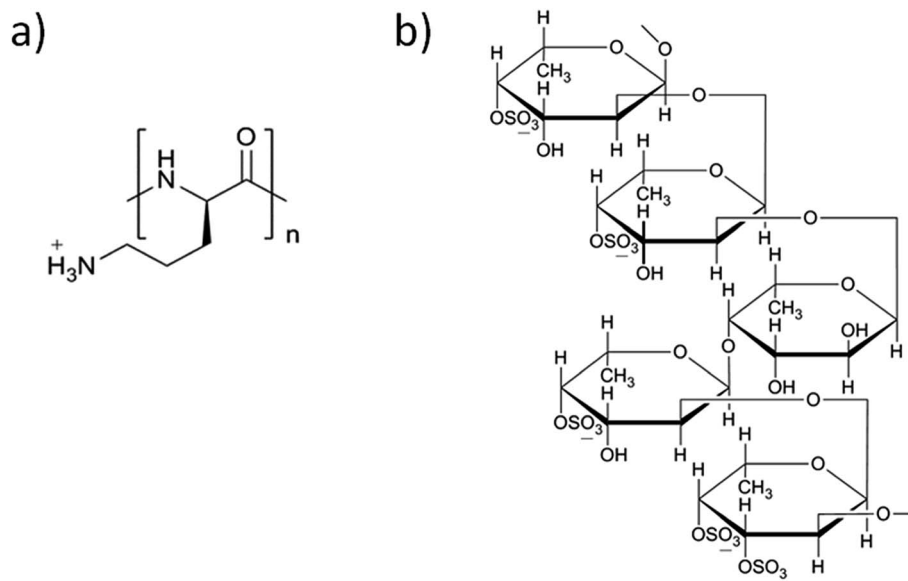


Fig. 1 Chemical structures of components of the shell (a) PLO and (b) fucoidan.

permeability.<sup>15,16</sup> Fucoidan (Fig. 1b) is another component of self-assembly, which contains L-fucose and sulfate groups.<sup>17,18</sup> This compound also possesses a variety of biological activities such as anti-coagulation, hypolipidemic, anti-tumor, anti-viral activity, and a property of strengthening the body's immune function.<sup>19–21</sup> Fucoidan induces the apoptosis in tumor cells<sup>22</sup> or affects the proliferation of tumor cells,<sup>23</sup> and could be used as potential anti-tumor drug to act against colon and breast cancers.<sup>24,25</sup>

Doxorubicin (DOX) is an anthracycline-based broad-spectrum anticancer drug, which is widely used against various malignancies such as liver, lung, breast, and ovarian cancers. However, higher doses or frequency of administration resulted in toxic side effects associated with heart and digestive tract.<sup>26</sup> To overcome this limitation, we designed a delivery system using polymers possessing anti-proliferative ability with the minimal amount of drug. Herewith, we demonstrated the encapsulation of anti-tumor drug DOX in a highly biocompatible and biodegradable PLGA nano-core for better performance using the emulsion solvent evaporation method. Subsequently, the shell deposited surrounding the nano-core comprises of polyelectrolytes, PLO as well as fucoidan, alternatively to prepare core-shell type PLGA-(PLO/fucoidan)<sub>n</sub> (Fig. 2a). Initially, the morphology and physico-chemical properties are

well characterized. Further, the DOX loading efficiency and its releasing profile are examined in LbL NPs (as shown in Fig. 2b). Later, the *in vitro* anti-proliferative ability of drug-loaded core-shell LbL NPs is investigated using breast cancer cell lines (MCF-7) as the tumor model. We anticipate that this innovative material design could provide a new chance and alternative option for the tough choices of LbL membrane materials, and the pharmacological properties of these materials would be beneficial for the effective treatment as interventional therapy in the future applications such as drug delivery system, surgical dressing, artificial skin, mucous membrane, degradable films, and others.

## 2. Materials and methods

### 2.1 Materials

Poly(lactide-co-glycolide) (PLGA) (D, L-lactide : glycolide = 50 : 50) with an average molecular weight of 70–100 KDa and poly-L-ornithine (molecular weight 30–70 KDa) were purchased from Sigma-Aldrich. Fucoidan was purchased from Shandong Jiejing Inc. Doxorubicin hydrochloride and bovine serum albumin (BSA) were obtained from Aladdin Co. Ltd. (China). The 4',6-diamidino-2-phenylindole dihydrochloride (DAPI) staining solution was purchased from Beijing Biodee Diagnostic Inc. Other chemicals were all obtained from Sinopharm Chemical Reagent Ltd. (China).

### 2.2 Preparation of PLGA NPs and DOX-PLGA NPs

PLGA NPs were prepared using O/W emulsion-solvent evaporation method as reported.<sup>27</sup> At first, PLGA (40 mg) was solubilized in dichloromethane (DCM), which acts as an oil phase in the design, alternatively BSA aqueous solution (8 mL) as the water phase. BSA acted as the surfactant (or stabilizer) for the emulsion process which could help the forming of PLGA NPs.

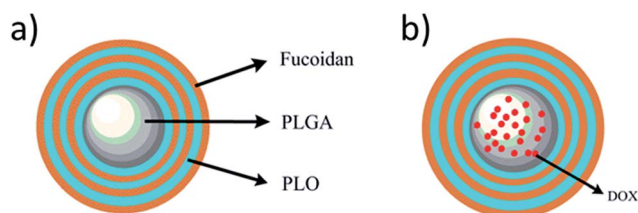


Fig. 2 Schematic representation of PLGA-(PLO/fucoidan)<sub>n</sub> nanoparticles (a) without and (b) with loading of DOX.



Later, the oil phase was added drop-wise to the water phase and subjected to the ultra-sonication (SCIENTZ, JY92-2D) for nano-emulsion preparation. Then, the mixed emulsion was poured into 200 mL of water and stirred for 3 h. Subsequently, the liquid organic phase was evaporated and the nanoparticles were washed repeatedly for 5 times by centrifuging at 10 000g, for 5 min.

Doxorubicin loaded PLGA NPs were prepared following similar procedure as described above. Initially, PLGA (60 mg) was dissolved in DCM (3 mL) with 0.6 mL of DOX solution (10 mg mL<sup>-1</sup> in methanol and chloroform mixture (1 : 1)). This solution was subsequently added drop-wise to 12 mL BSA in water, which was then emulsified by an ultrasonicator for 20 s. This emulsion was immediately poured into 300 mL of water and stirred for 3 h. The resulting particle suspension was purified *via* centrifugation (10 000g, 5 min) ahead of LbL assembly, eventually.

### 2.3 Preparation of PLGA-(PLO/fucoidan)<sub>4</sub> NPs (LbL NPs)

The PLO and fucoidan polymers were self-assembled layer upon a layer alternatively at a polyelectrolyte concentration of 1 mg mL<sup>-1</sup>. PLGA NPs/DOX-PLGA NPs (10 mg) as cores were added into 10 mL of polyelectrolyte solution subsequently one after the other through static adsorption, resulting in polyelectrolyte multi-layer films. The excess polyelectrolyte solution was washed-out using water. PLGA-(PLO/fucoidan)<sub>4</sub> NPs were prepared by repeating the process successively for multiple times. Herewith, we have repeated the layers for different times and the samples were named as PLGA-(PLO/fucoidan)<sub>0.5</sub> NPs, PLGA-(PLO/fucoidan)<sub>1</sub> NPs, PLGA-(PLO/fucoidan)<sub>1.5</sub> NPs, *etc.* Similarly, the DOX-PLGA NPs were also prepared following the above process to deposit multi-layered polymers. The whole processing steps of LbL NPs formation were illustrated in Fig. 3.

### 2.4 Microstructure and phase analyzing behavior study

The extensive morphological study of freeze-dried PLGA NPs and PLGA-(PLO/fucoidan)<sub>4</sub> NPs was performed by transmission

electron microscope (TEM, TEM 8400S, Shimadzu, Japan). Prepared nanoparticles (from PLGA cores to PLGA-(PLO/fucoidan)<sub>10</sub> NPs), each successive bilayer nanoparticles were homogeneously dispersed in water for the dynamic light scattering (DLS) measurements and instantaneously zeta-potential values of subsequent LbL nanoparticles (from PLGA NPs to PLGA-(PLO/fucoidan)<sub>5</sub> NPs) after each PLO or fucoidan layer was also observed.

### 2.5 *In vitro* drug loading and drug release study

The DOX loading efficiency of various nanoparticle formulations was tested by following the procedure below. Initially, 5 mg of NPs (DOX-PLGA NPs and DOX-PLGA-(PLO/fucoidan)<sub>4</sub> NPs) were loaded DOX in different drug dosage, 5 wt% (0.25 mg), 10 wt% (0.50 mg), 15 wt% (0.75 mg), respectively. At first, they were dissolved in DCM and appropriate amount of the phosphate buffered saline (PBS (pH-7.4)) solution was added and mixed under stirring until DCM volatilize completely. The remaining mixture was filtered using 0.22 μm membrane, and diluted appropriately. The absorbance of the resulting solution was recorded eventually using UV-Vis spectrophotometer, compared with PBS as blank. The experiment was performed in triplicate.

In a typical *in vitro* drug release study, 1.0 mg of doxorubicin equivalent amount was set as a baseline, according to the actual drug loading efficiency of nanoparticles. For an instance, according to the optimum drug loading condition, DOX loaded PLGA NPs and PLGA-(PLO/fucoidan)<sub>4</sub> NPs and 1.0 mg of pure DOX were suspended separately in 30 mL of PBS, mounted in dialysis bags, maintained at 37 °C and stirred at 60 RPM. Sampling was done by taking 3 mL of PBS from the dialysis bag at various time intervals (0.5, 1, 2, 3, 4, 6, 9, 12, 24, 36, 48, and 72 h) and the study continued by replacing the simulated fluids at the respective time intervals. The cumulative release percentage was calculated by measuring the drug concentration in the solution phase periodically using UV-Vis spectrophotometer.

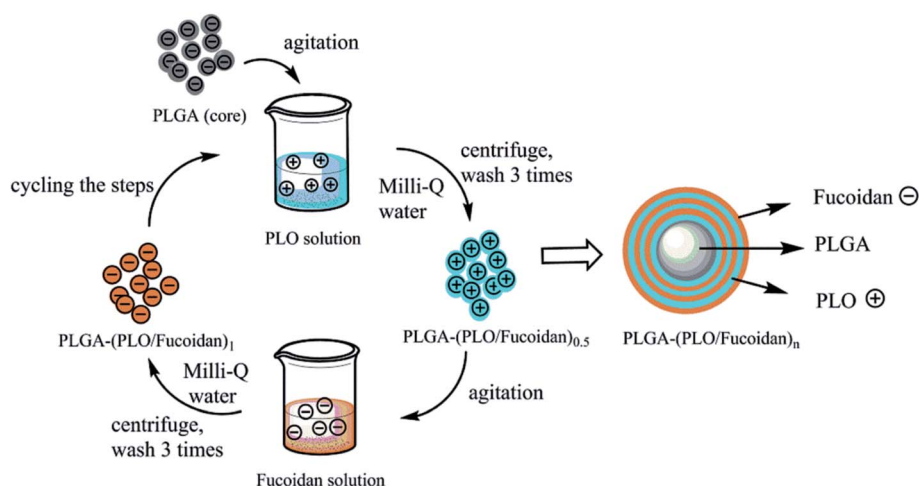


Fig. 3 Schematic illustration of preparation steps of PLGA-(PLO/fucoidan)<sub>n</sub> nanoparticles by ultrasonic emulsification of LbL self-assembly.



## 2.6 *In vitro* anti-tumor activity

Breast cancer cells (MCF-7 cell line, supplied by Institute of cell resource center, Chinese academy of sciences, Shanghai) were cultured in a DMEM medium supplemented with 10% FBS. Cells were seeded at a density of  $5 \times 10^5$  cells per well into 96-well plates and incubated for 48 hours in 5% CO<sub>2</sub> at 37 °C. After cells adhering, the medium was removed, and 100  $\mu$ L (1, 5, 10, 25, 50  $\mu$ g mL<sup>-1</sup>) of DOX-PLGA NPs and DOX-PLGA-(PLO/fucoidan)<sub>4</sub> NPs (which were prepared in the optimum drug loading condition) suspended in culture medium was added to substantiate the dose-dependent toxicity. After 24 h of incubation, the absorbance of cells was observed following the manufacturer's instructions of CCK-8 kit. In addition, time-dependent cytotoxicity study was performed by adding 100  $\mu$ L of 5  $\mu$ g mL<sup>-1</sup> drug loading PLGA NPs and PLGA-(PLO/fucoidan)<sub>4</sub> NPs suspension in the culture medium and incubated for 24, 48, and 72 h. Similarly, the results were recorded following the above procedure.

## 2.7 CLSM imaging

Cell internalization of design nanoconstructs was traced using CLSM imaging. MCF-7 cells were seeded at a density of  $5 \times 10^5$  cells per well, placing glass cover slips on a confocal laser plate and allowed to adhere for 48 h. Later, the medium was removed and 3 mL of 5  $\mu$ g mL<sup>-1</sup> of DOX-PLGA-(PLO/fucoidan)<sub>4</sub> NPs (in the optimum drug loading condition) suspended in culture

medium was added. After respective time intervals (0.5, 2, and 4 h) of incubation, the medium was removed and cells were washed with cold PBS and fixed using paraformaldehyde for 15 min. Cells were then washed again with PBS, and then one drop of DAPI solution was added onto the glass cover slips in confocal laser plates. Confocal laser scanning fluorescence imaging was performed with a Zeiss LSM710 confocal microscope (Carl Zeiss Microscopy GmbH Jena, Germany) to capture images.

## 3. Results and discussion

### 3.1 The morphology of PLGA NPs and PLGA-(PLO/fucoidan)<sub>4</sub> NPs

From the TEM images shown in Fig. 4, it is evident that the PLGA core nanoparticle was more or less spherical in shape (Fig. 4a). After self-assembling of polyelectrolyte materials, the surface became a bit irregular, which confirmed the external shallow shell (Fig. 4b). The particle size of various designed nanocarriers was obtained by the nano measurer software analysis, where PLGA core size was recorded as 112 nm. Meanwhile, after the self-assembly process, the particle size was increased to a range of 165–180 nm (Fig. 4b), which is suitable for ease of cell internalization, Fig. 4c had shown that the dispersed LbL NPs resulted in the detached polyelectrolyte layers due to ultrasonic treatment subsequently for each coating. However, no significant reduction in the size of the LbL

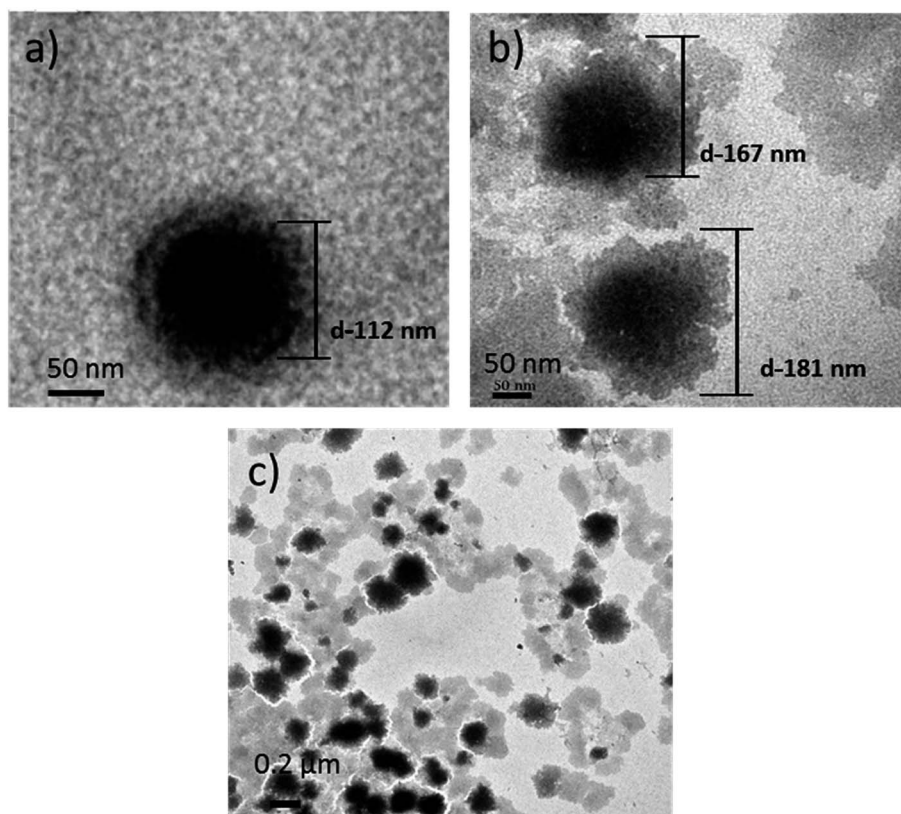


Fig. 4 TEM images of (a) PLGA NPs (scale bar-50 nm); (b) PLGA-(PLO/fucoidan)<sub>4</sub> NPs (scale bar-50 nm); (c) PLGA-(PLO/fucoidan)<sub>4</sub> (scale bar-0.2  $\mu$ m).



NPs was eventually observed. Comparing with the report of Romero,<sup>27</sup> who used the emulsified volatile method to prepare PLGA nanoparticles and Ramasamy,<sup>28</sup> who elucidated the morphology of self-assembly nanoparticles, it was similar representing the external irregular polyelectrolyte coatings, however the undesirable aggregation was not perceived.

### 3.2 Size distribution of PLGA NPs and PLGA-(PLO/fucoidan)<sub>4</sub> NPs

The particle size distributions of the designed PLGA NPs and self-assembled bilayers (PLGA-(PLO/fucoidan)<sub>n</sub>) on the surface are shown in Fig. 5. The average particle size of PLGA cores was 110 nm, with the increasing layer number, particle size increased gradually. After assembling of 4 bilayers, particle size was 170 nm, which increased to 299 nm after the assembly of 10 bilayers membrane. The data represents that the average size of each bilayer membrane was ~19 nm, whereas the poly(styrenesulfonate)/polyvinylpyrrolidone films prepared by Strydom group<sup>29</sup> resulted in  $9 \pm 1$  nm bilayer membrane size. The larger size might have resulted because of hydration of NPs,<sup>27</sup> since the particles were dispersed in water medium during DLS recordings, and other assumption might be the variations in polyelectrolyte, which also result in size disparity. However, as a drug delivery carrier, the layer number of assembly could satisfy the specific requirements with respective to controlled drug delivery and anti-proliferative activity. These DLS recordings were in agreement with the TEM measurements.

### 3.3 Zeta ( $\zeta$ )-potential measurements

After depositing the different polyelectrolyte alternatively to form a nano single-layer film, the charge was flipped for each step, as shown in Fig. 6. The average surface  $\zeta$ -potential of PLGA NPs cores was  $-25 \pm 1$  mV, while of the positive potential was  $+30 \pm 2$  mV and the negative potential was  $-24 \pm 2$  mV, which represented that the polyelectrolyte membranes had good

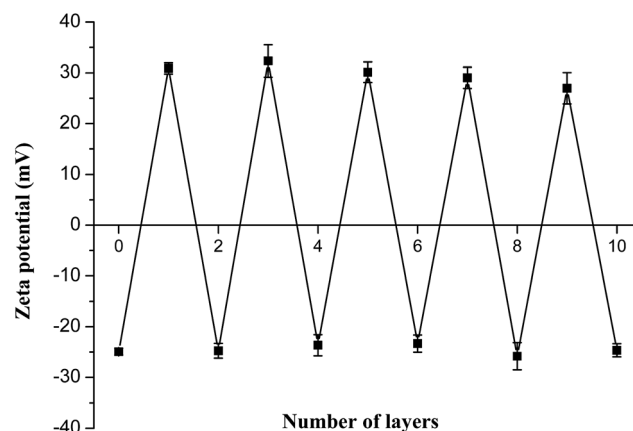


Fig. 6 The zeta potential values of PLGA-(PLO/fucoidan)<sub>n</sub> after deposition of each PLO or fucoidan layer.

stability with consistency in this system and the results were in agreement with the reports published elsewhere.<sup>30,31</sup>

### 3.4 In vitro drug loading and drug release study

The results of drug loading and encapsulation efficiency were shown in Fig. 7. The optimal drug loading conditions were optimized by altering the conditions such as increasing in drug amount (5 wt%, 10 wt%, 15 wt%), in both DOX-PLGA NPs and DOX-PLGA-(PLO/fucoidan)<sub>4</sub> NPs. The results showed that the drug loading amount increased with the increase of drug amount. However, the encapsulation efficiency decreased gradually. The DOX loading amount in PLGA NPs at various drug amounts was 3.9%, 6.8%, and 8.6% respectively, while in LbL NPs, it was 2.1%, 3.5%, and 4.8%. The encapsulation efficiency of DOX-PLGA NPs was 81.4%, 72.6%, 63.1%, DOX-PLGA-(PLO/fucoidan)<sub>4</sub> NPs was 42.5%, 36.6%, 33.7%, when the DOX was fed as the ratio of 5 wt%, 10 wt%, 15 wt% the NPs, respectively. PLGA NPs and LbL NPs with 10 wt% of DOX were used in further experiments.

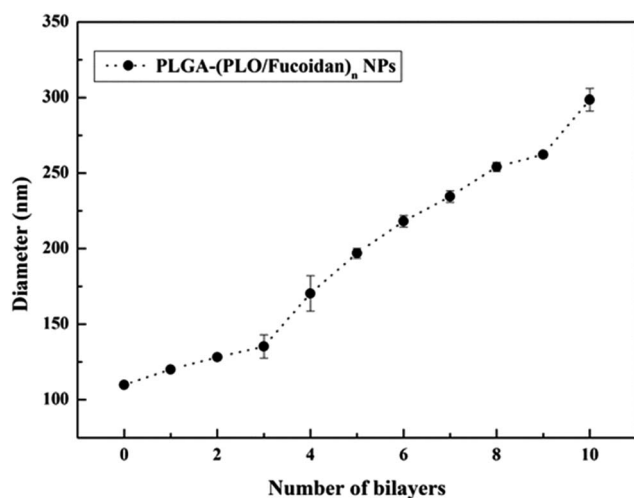


Fig. 5 The growth curve with respective to size of LbL NPs after depositing PLO and fucoidan alternatively.

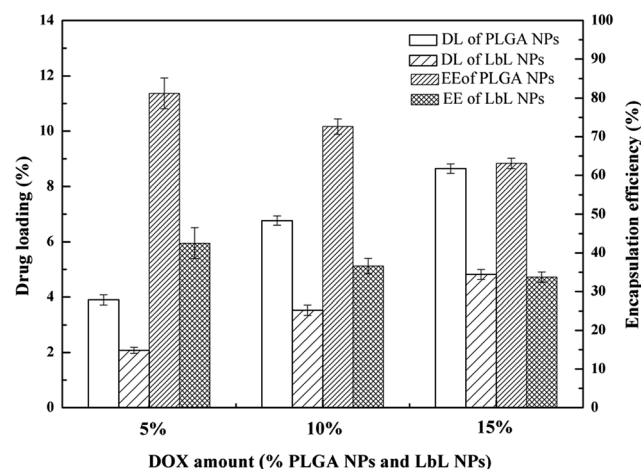


Fig. 7 Drug loading and encapsulation efficiency of PLGA NPs and PLGA-(PLO/fucoidan)<sub>4</sub> NPs.



The optimized formulation 10 wt% of drug loading PLGA NPs and PLGA-(PLO/fucoidan)<sub>4</sub> NPs were selected for *in vitro* cumulative drug release study and the cumulative release profile was represented in Fig. 8, Fig. 8a showed 0–72 h drug releasing effect, while Fig. 8b is 0–12 h releasing effect. The drug releasing rate of raw DOX was 80.9% after 6 h of incubation. PLGA NPs and LbL NPs have shown sustained-release patterns, despite the fact that there was no burst release in either of the nanoparticle formulations. The release of DOX encapsulated in the inner core was more sustained in LbL NPs because of the external multilayered polyelectrolyte shell, which means with the time increasing, DOX released slowly from the inner cores. The drug release was only 3.3% after 0.5 h, however the drug cumulative release was 57.9% after 36 h of incubation, and in agreement with the previous report. A few part of DOX remained in polyelectrolyte materials when releasing from the cores, which would not be tested by ultraviolet spectrum. After 72 h, the total releasing rate is still under than 60%, compared with

the result.<sup>32</sup> Because the remained DOX was still loaded in the inner cores, different polyelectrolyte materials and the number of coats in core-shell design might influence or decide the drug release ability.

### 3.5 *In vitro* anti-tumor activity

To evaluate the cytotoxicity of various nanoparticle formulations DOX-PLGA NPs and DOX-PLGA-(PLO/fucoidan)<sub>4</sub> NPs (DOX concentration equivalent to 5  $\mu\text{g mL}^{-1}$ ) along with the free DOX (5  $\mu\text{g mL}^{-1}$ ), we observed the cell morphology as well as measured the inhibition rate of NPs treatment in the MCF-7 cells. Images of cell morphology were captured after incubation with respective treatments for 72 h, as shown in Fig. 9. It is clear from the images that the DOX loaded NPs (Fig. 9c and d) as well as free DOX (Fig. 9b) treatment resulted in shrunken morphology, with reduced cell density at the magnified scale compared to the control group, *i.e.*, no treatment group

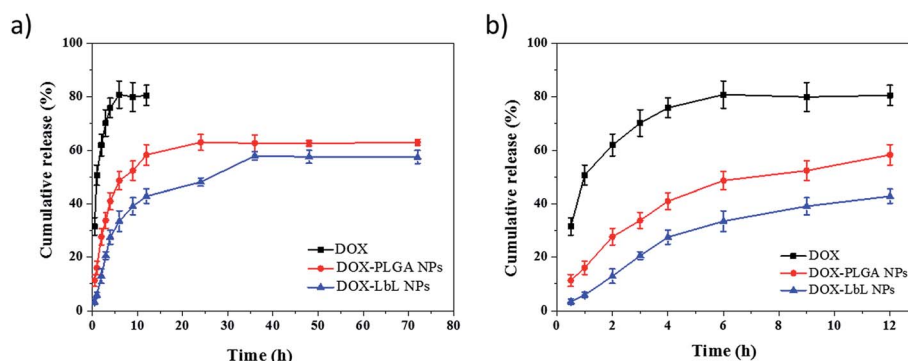


Fig. 8 The *in vitro* release profiles of 10 wt% drug-dosage nanoparticles. (a) 0–72 h; (b) 0–12 h.

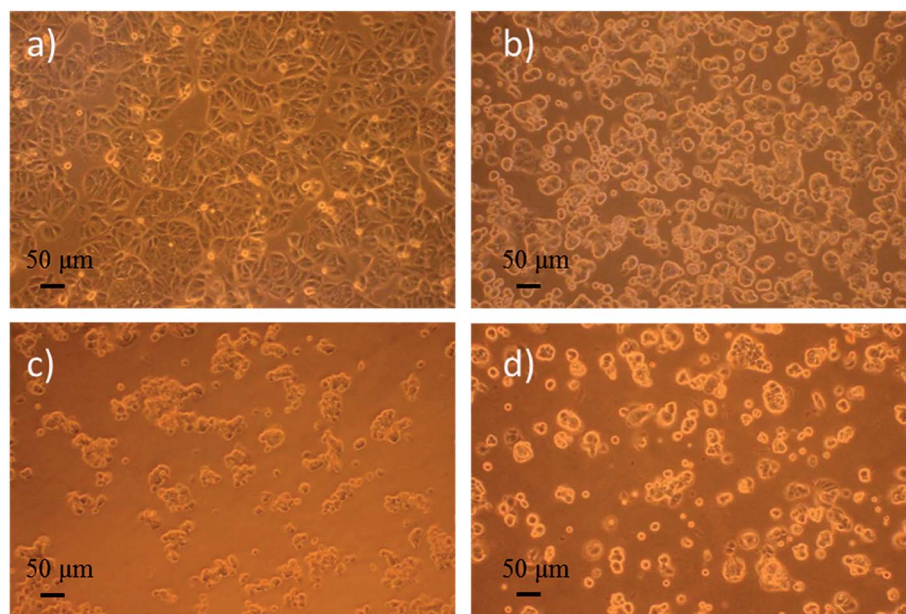


Fig. 9 Optical microphotograph of MCF-7 cells cultured with the drug concentration of 5  $\mu\text{g mL}^{-1}$  for 72 h. (a) fresh medium (control), (b) DOX, (c) DOX-PLGA NPs, (d) DOX-PLGA-(PLO/fucoidan)<sub>4</sub> NPs.



(Fig. 9a), where cells grew well, with circular or elliptic and large in size. This typical experiment demonstrated that nanoparticles treatment were comparatively more effective than the free DOX treatment group.

Anti-proliferative screening was performed using CCK-8 kit, a sensitive colorimetric assay to epitomize the inhibition results of DOX, DOX-PLGA NPs and DOX-PLGA-(PLO/fucoidan)<sub>4</sub> NPs co-cultured with MCF-7 cells (Fig. 10). The detection sensitivity of this kit is higher than other tetrazolium salts. We have performed both dose as well as time dependent inhibition rate, with increasing doses (1, 5, 10, 25, and 50  $\mu\text{g mL}^{-1}$ ) of DOX, DOX-PLGA NPs and DOX-PLGA-(PLO/fucoidan)<sub>4</sub> NPs (Fig. 10a) along with time of treatment exposure 24 h. Free DOX, DOX-PLGA NPs, and DOX-PLGA-(PLO/fucoidan)<sub>4</sub> NPs (DOX concentration equivalent to 5  $\mu\text{g mL}^{-1}$  in NPs) were selected for different time treatments (24, 48, and 72 h) (Fig. 10b), respectively. We observed the significant inhibition with the increasing concentration of NPs and free DOX, the reason behind the cell apoptosis might be the synthesis of RNA and DNA of tumor cells were inhibited by DOX.<sup>26</sup> Similarly, the time of exposure has also influenced the inhibition rate, *i.e.*, the cell inhibition rate increased with the increase in time of exposure, this might be due to the controlled delivery of DOX from NPs with the elapsing time. In time dependent experiments, 72 h of inhibition effect was lower in free DOX. Since DOX delivered from NPs were more effective with elapsed time than free DOX, due to ease of internalization of nanoparticles might be through endocytosis and sustained release of drug molecules from PLGA-(PLO/fucoidan)<sub>4</sub> nanocarriers. This is mandatory that increasing NPs concentration around tumor could certainly have a chance to kill cells.

### 3.6 Cellular uptake study

It is advantageous that DOX emits red fluorescence, where cellular internalization can be traced making use of this benefit. We performed cellular uptake study to trace DOX-PLGA NPs and DOX-PLGA-(PLO/fucoidan)<sub>4</sub> NPs co-cultured with MCF-7 cells for 0.5, 2, 4 h using CLSM, as shown in Fig. 11. The experiment

setup possessed two channels, *i.e.*, a DAPI channel for visualizing nucleus (blue in color) and a DOX channel for tracing nanocarriers (red in color), in addition the merged images were also displayed to analyze the close association. This concomitant state that DOX interacted with the cellular components might result in the cell apoptosis. The short time of treatment (*i.e.*, 0.5 h) (Fig. 11a–c) evidenced that the administered NPs were very close proximity, ready to internalize, and the same was achieved by a few of the NPs after 2 hours (Fig. 11d–f). In addition, after 4 hours of treatment, the images represented that the internalized NPs were ample higher and very close proximity to the nucleus, even contemporaneous intra-nuclear (Fig. 11g–i). These results supports the evidence to the inhibition rate of NPs (Fig. 10).

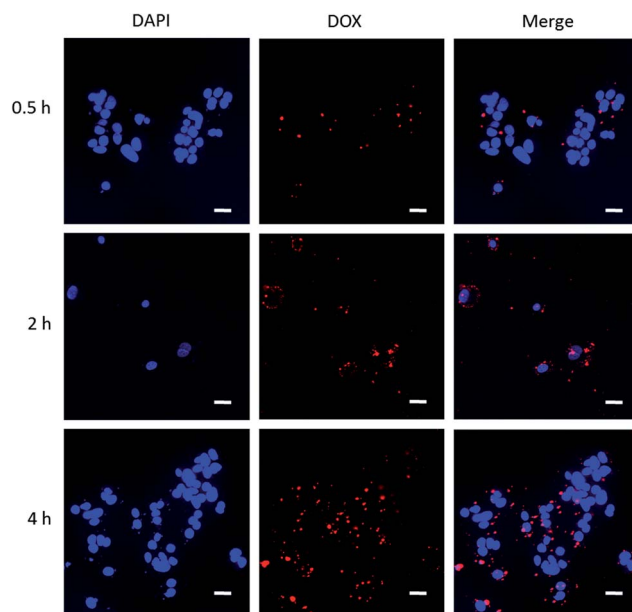


Fig. 11 CLSM images of cellular uptake of DOX-LbL NPs at various time intervals (scale bar-20  $\mu\text{m}$ ).

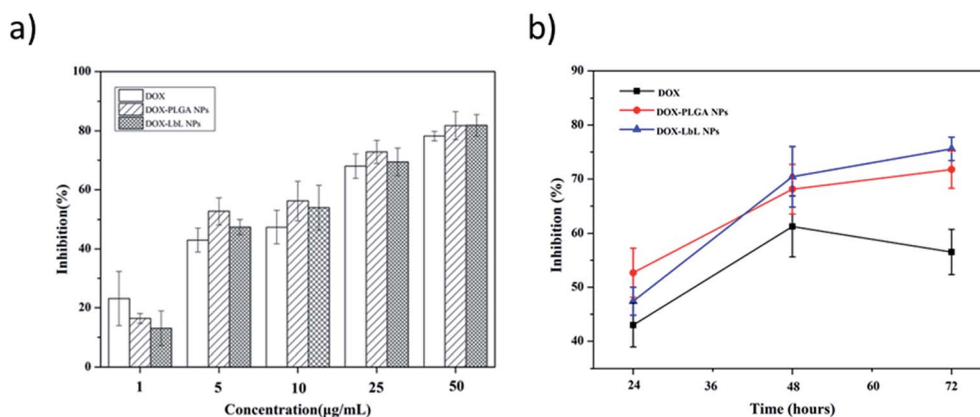


Fig. 10 The effect of concentration and treatment time of DOX, DOX-PLGA NPs, DOX-LbL NPs on the growth of MCF-7 cells. (a) Inhibition of MCF-7 cells subjected to various treatments at different concentrations for 24 h (1, 5, 10, 25, 50  $\mu\text{g mL}^{-1}$ ); (b) inhibition of MCF-7 cells subjected to various treatment at different exposure time interval (24, 48, and 72 h), (DOX was added in the same concentration (5  $\mu\text{g mL}^{-1}$ ) compared to the other groups).



## 4. Conclusion

In summary, we prepared PLGA cores using O/W emulsion solvent evaporation method and subsequently, PLGA-(PLO/fucoidan)<sub>n</sub> ( $n = 0.5, 1, 1.5, \dots, 10$ ) NPs were prepared by the LbL self-assembly technique for the preparation of composite films of polyelectrolytes (PLO, fucoidan) on the surface of PLGA cores deposited alternatively. Doxorubicin loaded in the PLGA-(PLO/fucoidan)<sub>4</sub> NPs possessed good sustained drug release ability and ease of cell internalization capability, which have shown an outstanding ability to kill breast tumor cells. These innovative LbL NPs possessing high anti-tumor efficacy could be used as a potential drug delivery vehicle and advantageous over other nanocarriers in medicine.

## Acknowledgements

Financial supports from NSFC (31000441 and 31170939), the National marine economic innovation and development project (16PYY007SF17), the Science Research Foundation of National Health and Family Planning Commission of PRC & United Fujian Provincial Health and Education Project for Tracking the Key Research (WKJ-2016-2-22), the Program for New Century Excellent Talents in Fujian Province University (2014FJ-NCET-ZR01) and the Promotion Program for Young and Middle-aged Teacher in Science and Technology Research of Huaqiao University (ZQN-PY108) are gratefully acknowledged. We also kindly thank Prof. Nicholas Kotov (University of Michigan) for giving suggestions to our manuscript.

## References

- 1 S. Correa, E. C. Dreaden, L. Gu and P. T. Hammond, Engineering nanolayered particles for modular drug delivery, *J. Controlled Release*, 2016, **240**, 364–386.
- 2 N. A. Kotov, I. Dekany and J. H. Fendler, Layer-by-layer self-assembly of polyelectrolyte-semiconductor nanoparticle composite films, *J. Phys. Chem.*, 1995, **99**, 13065–13069.
- 3 G. Decher, Fuzzy nanoassemblies: toward layered polymeric multicomposites, *Science*, 1997, **277**, 1232–1237.
- 4 M. M. de Villiers, D. P. Otto, S. J. Strydom and Y. M. Lvov, Introduction to nanocoatings produced by layer-by-layer (LbL) self-assembly, *Adv. Drug Delivery Rev.*, 2011, **63**, 701–715.
- 5 T. Boudou, T. Crouzier, K. Ren, G. Blin and C. Picart, Multiple functionalities of polyelectrolyte multilayer films: new biomedical applications, *Adv. Mater.*, 2010, **22**, 441–467.
- 6 P. T. Hammond, Engineering materials layer-by-layer: challenges and opportunities in multilayer assembly, *AIChE J.*, 2011, **57**, 2928–2940.
- 7 Z. Liang, K. Bernardino, J. Han, Y. Zhou, K. Sun, A. F. de Moura and N. A. Kotov, Optical anisotropy and sign reversal in layer-by-layer assembled films from chiral nanoparticles, *Faraday Discuss.*, 2016, **191**, 141–157.
- 8 M. Keeney, X. Y. Jiang, M. Yamane, M. Lee, S. Goodman and F. Yang, Nanocoating for biomolecule delivery using layer-by-layer self-assembly, *J. Mater. Chem. B*, 2015, **3**, 8758–8770.
- 9 H. Ge, L. Tan, P. Wu, Y. Yin, X. Liu, H. Meng, G. Cui, N. Wu, J. Lin, R. Hu and H. Feng, Poly-L-ornithine promotes preferred differentiation of neural stem/progenitor cells *via* ERK signalling pathway, *Sci. Rep.*, 2015, **5**, 15535.
- 10 Y. Kamiya, T. Yamaki, M. Uchida, T. Hatanaka, M. Kimura, M. Ogihara, Y. Morimoto and H. Natsume, Preparation and evaluation of PEGylated poly-L-ornithine complex as a novel absorption enhancer, *Biol. Pharm. Bull.*, 2017, **40**, 205–211.
- 11 I. J. Wajszon, L. A. de Carvalho, A. Biancalana, W. A. da Silva, C. Dos Santos Mermelstein, E. G. de Araujo and S. Allodi, Culture of neural cells of the eyestalk of a mangrove crab is optimized on poly-L-ornithine substrate, *Cytotechnology*, 2016, **68**, 2193–2206.
- 12 M. S. Liberio, M. C. Sadowski, C. Soekmadji, R. A. Davis and C. C. Nelson, Differential effects of tissue culture coating substrates on prostate cancer cell adherence, morphology and behavior, *PLoS One*, 2014, **9**, e112112.
- 13 S. Balaji, Y. Zhou, A. Ganguly, E. C. Opara and S. Soker, The combined effect of PDX1, epidermal growth factor and poly-L-ornithine on human amnion epithelial cells' differentiation, *BMC Dev. Biol.*, 2016, **16**, 8.
- 14 H. Ge, A. Yu, J. Chen, J. Yuan, Y. Yin, W. Duanmu, L. Tan, Y. Yang, C. Lan, W. Chen, H. Feng and R. Hu, Poly-L-ornithine enhances migration of neural stem/progenitor cells *via* promoting  $\alpha$ -actinin 4 binding to actin filaments, *Sci. Rep.*, 2016, **6**, 37681.
- 15 S. K. Tam, S. Bilodeau, J. Dusseault, G. Langlois and J. P. Halle, Biocompatibility and physicochemical characteristic of alginate-polycation microcapsules, *Acta Biomater.*, 2011, **7**, 1683–1692.
- 16 M. D. Darrabie, W. F. Kendall Jr and E. C. Opara, Characteristic of poly-L-ornithine-coated alginate microcapsules, *Biomaterials*, 2005, **26**, 6845–6852.
- 17 Z. Zhang, K. Teruya, T. Yoshida, H. Eto and S. Shirahata, Fucoidan extract enhances the anti-cancer activity of chemotherapeutic agents in MDA-MA-231 and MCF-7 breast cancer cells, *Mar. Drugs*, 2013, **11**, 81–89.
- 18 S. Shirahata, Z. Zhang, T. Yoshida, H. Eto and K. Teruya, Fucoidan extract enhances the anti-cancer activity of chemotherapeutic agents in breast cancer cells, *BMC Proc.*, 2013, **7**, 70.
- 19 G. Mossavou, D. H. Kwak, B. W. Obiang-Obonou, C. A. Maranguy, S. D. Dinzouna-Boutamba, D. H. Lee, O. G. Pissibanganga, K. Ko, J. I. Seo and Y. K. Choo, Anticancer effects of different seaweeds on human colon and breast cancers, *Mar. Drugs*, 2014, **12**, 4898–4911.
- 20 J. H. Fitton, Therapies from fucoidan; multifunctional marine polymers, *Mar. Drugs*, 2011, **9**, 1731–1760.
- 21 B. Lowe, J. Venkatesan, S. Anil, M. S. Shim and S. K. Kim, Preparation and characterization of chitosan-natural nano hydroxyapatite-fucoidan nanocomposites for bone tissue engineering, *Int. J. Biol. Macromol.*, 2016, **93**, 1479–1487.
- 22 T. V. Alekseyenko, S. Y. Zhanayeva, A. A. Venediktova, T. N. Zvyagintseva, T. A. Kuznetsova, N. N. Besednova and T. A. Korolenko, Anti-tumor and antimetastatic activity of fucoidan, a sulfated polysaccharide isolated from the



- Okhotsk Sea *Fucus evanescens* brown alga, *Bull. Exp. Biol. Med.*, 2007, **143**, 730–732.
- 23 C. Oliveira, A. S. Ferreira, R. Novoa-Carballal, C. Nunes, I. Pashkuleva, N. M. Neves, M. A. Coimbra, R. L. Reis, A. Martins and T. H. Silva, The key role of sulfation and branching on fucoidan antitumor activity, *Macromol. Biosci.*, 2017, **17**, 1600340.
  - 24 F. Atashrazm, R. M. Lowenthal, G. M. Woods, A. F. Holloway and J. L. Dickinson, Fucoidan and cancer: a multifunctional molecule with anti-tumor potential, *Mar. Drugs*, 2015, **13**, 2327–2346.
  - 25 L. Wu, J. Sun, X. Su, Q. Yu, Q. Yu and P. Zhang, A review about the development of fucoidan in antitumor activity: Progress and challenges, *Carbohydr. Polym.*, 2016, **154**, 96–111.
  - 26 D. Agudelo, P. Bourassa, G. Berube and H. A. Tajmir-Riahi, Review on binding of anticancer drug doxorubicin with DNA and tRNA : structure models and antitumor activity, *J. Photochem. Photobiol., B*, 2016, **158**, 274–279.
  - 27 G. Romero, I. Estrela-Lopis, J. Zhou, E. Rojas, A. Franco, C. S. Espinel, A. G. Fernandez, C. Gao, E. Donath and S. E. Moya, Surface engineered poly(lactide-co-glycolid) nanoparticles for intracellular delivery: uptake and cytotoxicity-a confocal Raman microscopic study, *Biomacromolecules*, 2010, **11**, 2993–2999.
  - 28 T. Ramasamy, Z. S. Haidar, T. H. Tran, J. Y. Choi, J. H. Jeong, B. S. Shin, H. G. Choi, C. S. Yong and J. O. Kim, Layer-by-layer assembly of liposomal nanoparticles with PEGylated polyelectrolytes enhances systemic delivery of multiple anticancer drugs, *Acta Biomater.*, 2014, **10**, 5116–5127.
  - 29 S. J. Strydom, D. P. Otto, W. Liebenberg, Y. M. Lvov and M. M. de Villiers, Preparation and characterization of directly compactible layer-by-layer nanocoated cellulose, *Int. J. Pharm.*, 2011, **404**, 57–65.
  - 30 Z. Poon, J. B. Lee, S. W. Morton and P. T. Hammond, Controlling *in vivo* stability and biodistribution in electrostatically assembled nanoparticles for systemic delivery, *Nano Lett.*, 2011, **11**, 2096–2103.
  - 31 E. C. Dreaden, S. W. Morton, K. E. Shopsowitz, J. H. Choi, Z. J. Deng, N. J. Cho and P. T. Hammond, Bimodal tumor-targeting from microenvironment responsive hyaluronan layer-by-layer (LbL) nanoparticles, *ACS Nano*, 2014, **8**, 8374–8382.
  - 32 S. W. Morton, Z. Poon and P. T. Hammond, The architecture and biological performance of drug-loaded LbL nanoparticles, *Biomaterials*, 2013, **34**, 5328–5335.

